The influence of the arc current on the cold electrode erosion

Alexei M. Essiptchouk, A. Marotta, and Leonid I. Sharakhovsky

Citation: Physics of Plasmas (1994-present) **10**, 3770 (2003); doi: 10.1063/1.1599856
View online: http://dx.doi.org/10.1063/1.1599856
View Table of Contents: http://scitation.aip.org/content/aip/journal/pop/10/9?ver=pdfcov
Published by the AIP Publishing

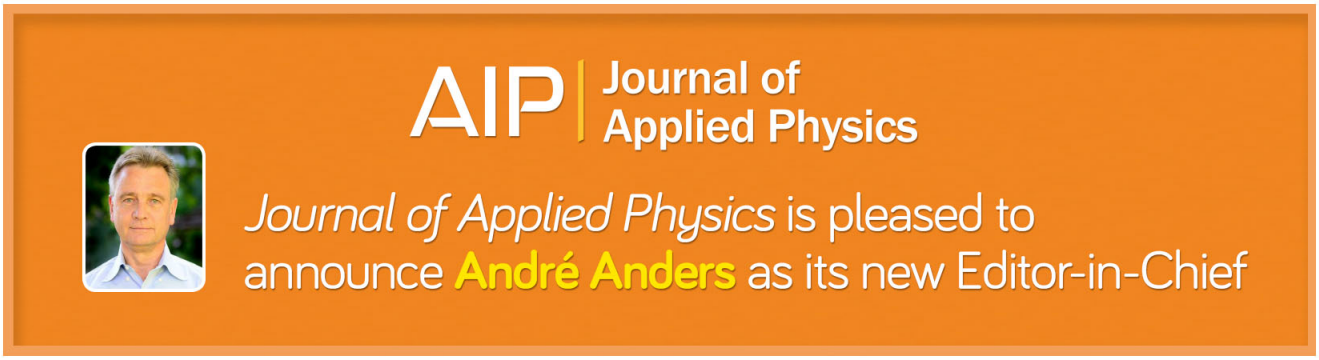

The influence of the arc current on the cold electrode erosion

Alexei M. Essiptchouk,[a] A. Marotta, and Leonid I. Sharakhovsky[a]
Instituto de Física "Gleb Wataghin," Universidade Estadual de Campinas, Unicamp, 13083-970, Campinas, São Paulo, Brazil

(Received 10 February 2003; accepted 18 June 2003)

A study of copper cathode erosion in a magnetically driven arc setup, as a function of arc current, is reported. The experiments showed the presence of two different erosion regimes. In the low current micro-erosion regime, erosion slowly rises with arc current. Then, at a certain critical current, macro-erosion begins, and has a strong dependence of erosion on current. It was shown that the critical current for transition from micro- to macro-erosion is a linearly decreasing function of the applied magnetic field. The erosion versus current behavior is shown to be explained by a recently published thermal model. © *2003 American Institute of Physics.*
[DOI: 10.1063/1.1599856]

I. INTRODUCTION

Cold cathode erosion is an important issue in all electric arc devices, as in gas blast circuit breakers and electric arc heaters (EAHs). Cold cathodes deserve more attention due to their much higher erosion than thermionic cathodes and cold anodes. Thermionic cathodes operate with motionless arc spots, while cold electrodes must operate under fast moving arc spots, provided by a magnetic field or a swirling gas, in order to prevent their fast destruction by erosion.

Many researchers (see Marotta[1] and references therein) have investigated cold cathode erosion under different operating conditions. Empirical power formulas of the type $g \propto I^a$ have been proposed[2,3] in the literature, with the exponent a between 2.24 and 4.5, depending on electrode surface conditions. An analysis of the erosion dependence on current was also attempted for a copper cathode.[4] However, no systematic investigations, based on any erosion model, were done. In this report, we study systematically the behavior of the copper cold cathode erosion as a function of the arc current.

In recently published papers,[1,5] a simple thermal model for cold electrode erosion was proposed, in which the arc current I, the electrode surface temperature T_0 and the arc spot velocity v are the main determining parameters for cold electrode erosion. Two idealized versions of the model were developed: one for a continuously moving arc spot with constant spot velocity v and another for a discontinuously (stepwise, jumping) moving arc spot. Depending on the values of current, electrode surface temperature and arc spot velocity, the electrode surface under the arc spot can reach the fusion temperature. If the fusion temperature under the spot is not reached, no erosion tracks are visible on the electrode surface. This is called the micro-erosion regime and occurs for low currents and electrode surface temperatures. On the contrary, strong erosion is observed (the macro-erosion regime) for high currents, when the cathode surface reaches fusion temperature. The experimental behavior for erosion versus current $g(I)$ will be shown in this report to be according to the above-mentioned thermal model. The experimental results were obtained in a coaxial magnetically driven arc setup, simulating an EAH.

II. THE EXPERIMENTAL SETUP

A steady-state coaxial experimental setup, with a magnetically driven arc, was used for the cathode erosion measurements (see Fig. 1). The system was equipped with water-cooled commercial copper-ring electrodes placed in an axial magnetic field. The outer electrode was the cathode, with $2R_1 = 40$ mm inner diameter and 5 mm width. It was isolated from the adjacent parts of the setup by thermal- and electro-insulating spacers. The working gas was air, operated with a pressure close to one atmosphere. It was supplied in the axial direction without vortex flow.

Current I, arc rotation velocity v, cathode surface temperature T_0, and the integral heat flux Q supplied to the cathode ring inner surface were recorded. The investigated cathode was placed inside a water-cooled ring jacket, embracing the cathode ring insert at its outer diameter. Most of the experiments were made with a cathode ring thickness of 10 mm (outer ring diameter of $2R_2 = 60$ mm). For safety purposes, the water-cooling flow rate was maintained constant. In order to increase the cathode surface temperature, some experiments were carried out with a different cathode ring, with $2R_2 = 120$ mm. After each 10 min arc experiment, the cathode ring insert was extracted from the cooled jacket and weighed to obtain the average mass erosion rate G $(\mathrm{kg\,s^{-1}})$.

The experiments were carried out for 4 different magnetic fields: $B = 0.01$; 0.137; 0.2; and 0.35 T. The arc current was varied in the range 95–480 A. The air and the jacket cooling water flow rates were maintained constant at $120\,\mathrm{l\,min^{-1}}$ and $4.4\,\mathrm{l\,min^{-1}}$, respectively. The axial gas velocity in the inter-electrode gap was $7.6\,\mathrm{m\,s^{-1}}$.

[a]Permanent address: The Luikov Heat & Mass Transfer Institute, P. Brovki street, 15, 220072, Minsk, Republic of Belarus.

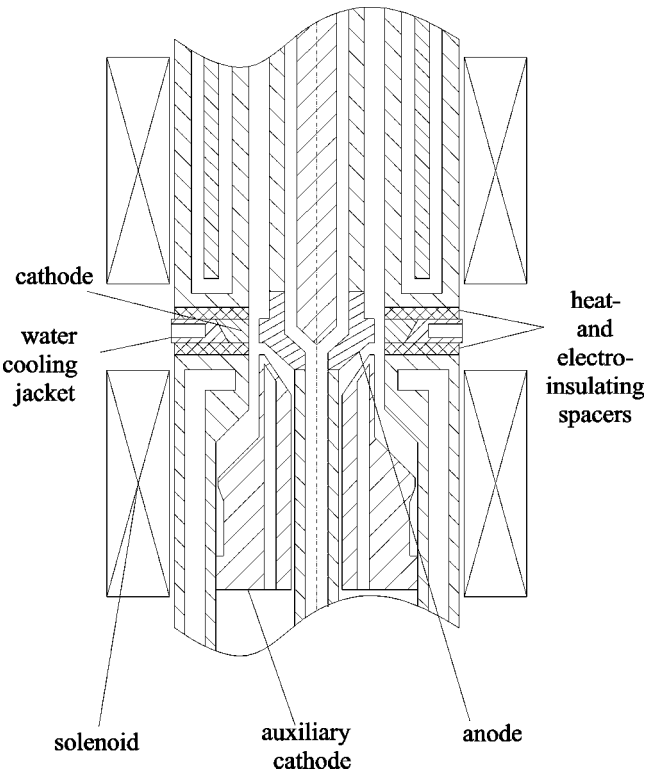

FIG. 1. Diagram of the experimental setup.

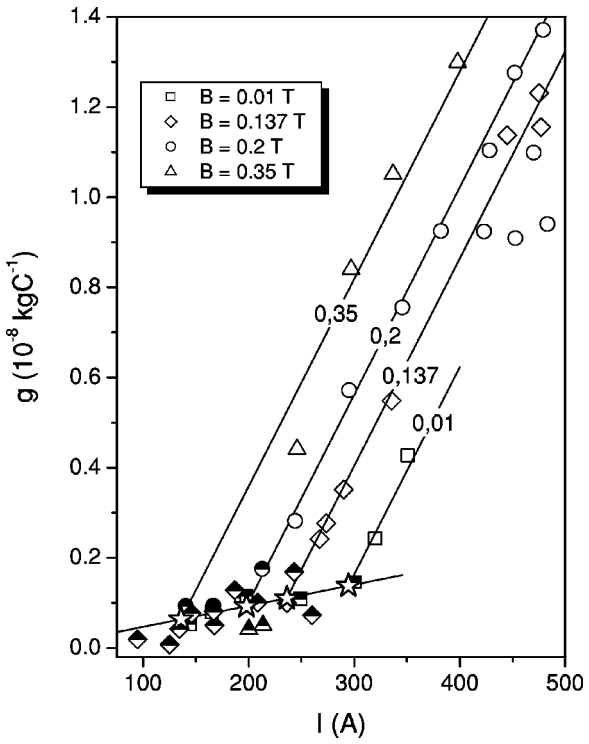

FIG. 2. Specific erosion g of a copper cathode versus current I, for a cathode with inner diameter $2R_1=40$ mm, outer diameter $2R_2=60$ mm and for four different magnetic field values. Lines are linear approximations of the experimental points for each value of B (shown). The half-painted points relate to the micro-erosion regime. The transition points from micro- to macro-erosion are marked by stars.

III. RESULTS AND DISCUSSION

Figure 2 shows the specific erosion rate g as function of current I, for the setup described above (cathode inner diameter $2R_1=40$ mm). We observe clearly in all plots a sudden increase of erosion at a critical current value I_{crit}. This critical current divides the plot in two parts: one with slowly increasing erosion and the other with a fast increase of erosion. The former will be called micro-erosion and the latter macro-erosion. We fitted the experimental points for each value of B, with two different linear functions $g(I)$ for the micro- and macro-erosion regions, respectively. We note that the slope dg/dI for the linear fits is identical for all magnetic fields—approximately as $4.68\times10^{-12}\ \mathrm{kg\,C^{-1}\,A^{-1}}$ for micro-erosion and as $4.6\times10^{-11}\ \mathrm{kg\,C^{-1}\,A^{-1}}$ for macro-erosion.

Figures 3(a) and 3(b) show, respectively, the critical erosion values g_{crit} and I_{crit} as functions of B, and a linear fit of each. As shown, g_{crit} and I_{crit} are decreasing functions of the magnetic field B, and can be represented in the form $I_{\mathrm{crit}}=I_{\mathrm{crit0}}-\delta B$ and $g_{\mathrm{crit}}=g_{\mathrm{crit0}}-\varepsilon B$, respectively. Here, for our experiments, and for constant experimental conditions, $I_{\mathrm{crit0}}=297.5$ A, $\delta=464.7\ \mathrm{A\,T^{-1}}$, $g_{\mathrm{crit0}}=1.39\times10^{-9}\ \mathrm{kg\,C^{-1}}$, $\varepsilon=2.2\times10^{-9}\ \mathrm{kg\,C^{-1}\,T^{-1}}$. For a given electrode and cooling regime, the copper cathode macro-erosion can be approximated with sufficient accuracy by a simple linear function of current with identical slopes for all magnetic field values: $g=g_{\mathrm{crit}}(B)+\gamma[I-I_{\mathrm{crit}}(B)]$, where $g_{\mathrm{crit}}(B)$ is the specific erosion at the critical current I_{crit} for each value of B and $\gamma=4.6\times10^{-11}\ \mathrm{kg\,C^{-1}\,A^{-1}}$.

Figure 4 shows the combined results of Fig. 2 (points inside the dotted frame), together with points, obtained on the same experimental setup as above, but using a cathode with a larger outer diameter of $2R_2=120$ mm and a magnetic field of 0.2 T. In this figure are also shown points, taken from a previous work,[5] obtained in a similar experimental setup using currents up to 1000 A, but with a cathode having an inner diameter of $2R_1=50$ mm and a magnetic field of 0.133 T, and points obtained on a cathode with an inner diameter of 90 mm and a magnetic field of 0.03 T. Again, the experimental points were approximated by linear fits.

The presence of the two different types of erosion behavior, shown in the figures above, can be explained by the cold electrode erosion thermal model.[1,5] The model is based on a nondimensional parameter $f=\tau_0/\tau_r$, where τ_0 is the time for a given point on the electrode surface to reach the fusion temperature T_f and τ_r is the residence time of that point under the arc spot. The value of f is given by the expression[1,5]

$$f=\frac{\pi^{1.5}v\lambda^2(T_f-T_0)^2}{8aj^{1.5}U^2I^{0.5}},$$

where I is the current, T_0 is the mean electrode surface temperature, v is the arc spot velocity, j and U are arc spot parameters—the effective arc spot current density and the thermal volt-equivalent, respectively, and λ and a are the thermal conductivity and diffusivity of the electrode material, respectively. Depending on the value of f two regimes

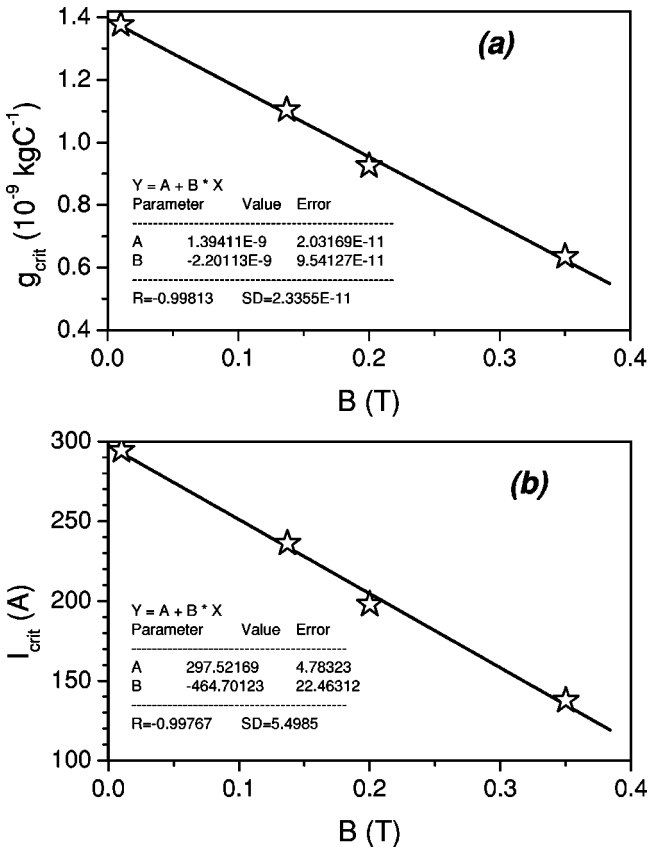

FIG. 3. (a), (b) Critical erosion g_{crit} (the transition from micro- to macro-erosion) and corresponding critical current I_{crit}, respectively, for points in Fig. 2, as function of the magnetic field, for a cathode with inner diameter $2R_1=40$ mm and outer diameter $2R_2=60$ mm. R is the correlation coefficient.

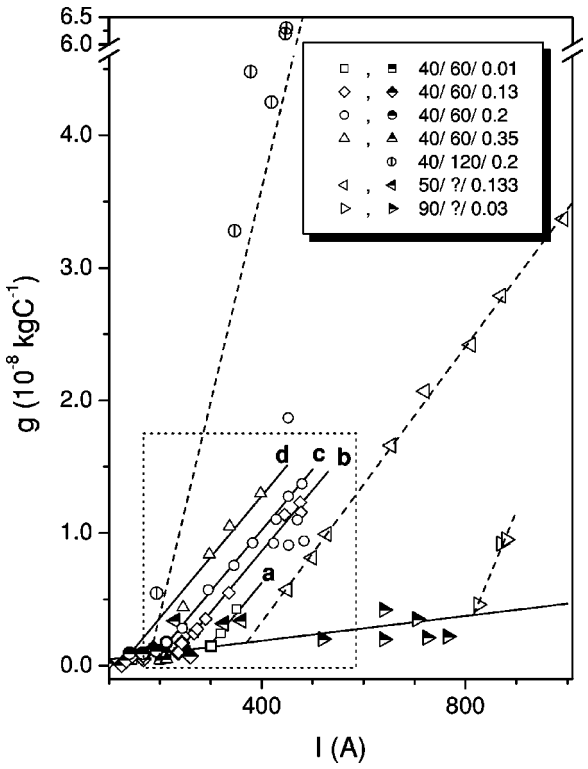

FIG. 4. Specific erosion g of copper cathode versus current I. Point specifications: $2R_1/2R_2/B$, where $2R_1$, $2R_2$ and B are the inner and outer cathode diameters (mm) and magnetic field strength (in Tesla). The question marks ("?") in the last two lines of the legend, for the inner cathode diameters 50 and 90 mm, means that we have no information about their outer diameters $2R_2$. Lines a, b, c, d: linear approximations to basic points from Fig. 2. The half-painted points relate to the micro-erosion regime.

of erosion can be obtained: one for $f>1$ (or $\tau_r<\tau_0$), called the micro-erosion regime, and another for $f<1$ (or $\tau_r>\tau_0$), called the macro-erosion regime.

The thermal model was developed for the macro-erosion regime. For certain values of current I, electrode surface temperature T_0 and spot velocity v, no points on the electrode surface under the spot area reach the fusion temperature T_f, no melting takes place and erosion $g=0$ (the micro-erosion regime). Thus, the model is not able to explain the small and almost constant value of micro-erosion g_0, which is observed experimentally, for small values of I and T_0. Then, at I_{crit}, $T_{0\text{crit}}$ and v_{crit}, the critical condition $f=1$ is reached and points on the electrode surface under the spot area attain the fusion temperature T_f and macro-erosion begins. With further increasing I and T_0, a strong increase in erosion is observed (the macro-erosion regime), as shown by Figs. 2 and 4.

Figures 3(a) and 3(b) are also explained by the thermal model. The increase of the magnetic field B causes an increase in the arc spot velocity v and arc spot parameters[6,7] j and U. This produces a transition from micro-erosion to macro-erosion at a lower current.

Figure 4 shows also that deterioration in the water cooling of the cathode inner surface, due to a thicker cooled wall, changes the erosion from micro- to macro-erosion at a lower critical current. Furthermore, the slope dg/dI of the macro-erosion regime is higher when cooling is less efficient (compare points with $2R_2=120$ mm in Fig. 4 with points with $2R_2=60$ mm).

The different power dependences of g vs I, published in the literature by different authors,[2,3] can be explained as a result of different efficiencies of heat transfer from the electrode surface to the electrode water-cooling system and also as a limitation due to disregarding the differences between micro- and macro-erosion regimes.

Many authors have shown that the arc spot in a cold cathode is composed of many, high current density (10^{10}–10^{12} A m^{-2}) micro-spots (see, e.g., Jüttner,[8] and references therein). Studying the internal structure of arc spots in vacuum, Rakhovsky[3] observed that, for one type of arc spots, which he called the "type I cathode spots," the micro-spots inside the larger spot act practically independently one of the other. Type I micro-spots are typical of low currents and low cathode temperatures, and are not followed by visible erosion traces on the electrode surface. The other type of arc spots, called by Rakhovsky "type II cathode spots," is typical of high currents and high cathode temperatures. Type II micro-spots behave collectively, with their thermal fields interacting between themselves. These micro-spots are followed by macroscopic melted areas on the cathode surface, which can be identified visually.

In contrast to vacuum arcs, the study of gaseous arc spot structures and micro-spots dynamics is difficult because of

the higher luminosity of the plasma column than the spots, so very little is found in the literature[8] about the micro-spot behavior in gaseous arcs. However, in atmospheric pressure as well as in vacuum, the arc spots on cold electrodes must provide for the transfer of current by the generation of a metal vapor. Coulombe and Meunier[9] found that high spot pressures, considerably exceeding the atmospheric pressure, are necessary to maintain high cold cathode spot current densities for gaseous arcs. Therefore, basic cathode spot processes in vacuum arcs, such as evaporation and current transfer, might be expected to be observed in gas arcs.[8] Extending this assumption to the spot structure, as described by Rakhovsky,[3] it can be suggested for atmospheric arcs that type I spots might also be found in the micro-erosion regime, and type II in the macro-erosion regime, the transition to type II occurring when the temperature under the spot reaches T_f.

Carrying out experiments in an EAH with tubular copper electrodes, erosion behavior very similar to Figs. 2 and 4 was observed,[10,11] with the presence of the two erosion branches, and a sharp increase of $g(I)$ for high currents (macro-erosion regime). High speed photography showed the appearance of cathodic jets only for the high current branch of $g(I)$. The authors explained this behavior by the destruction of the gas vortex that was utilized in their EAH to move the electric arc. This explanation is in contradiction with our experimental results obtained without a gas vortex, where the same effect of a sharp increase of erosion was observed. The existence of two different erosion regimes corroborates our observations and, furthermore, indicates that the macro-erosion regime can be accompanied by cathodic jets.

IV. CONCLUSION

We show in this report that, for a magnetically driven arc in a coaxial setup and for a given magnetic field value, the erosion rate as function of current can be approximated by two linear sections, with very different slopes. The low slope section micro-erosion regime occurs for low currents, while the high slope macro-erosion section occurs for high currents. The change from micro- to macro-erosion occurs at a certain critical current value, which is a decreasing function of magnetic field. The observed erosion behavior can be explained by a recently published thermal model, based on the fusion of the electrode surface under the spot area. On reaching the fusion temperature under the spot, a strong increase of erosion is observed, and the macro-erosion regime begins. Basic cathode spot processes in vacuum arcs, as described by Rakhovsky, might be expected to occur also in gas arcs, as type I cathode spots in the micro-erosion regime and type II in the macro-erosion regime. Some experimental results obtained by other authors show that the macro-erosion regime might be accompanied by cathodic jets. The slope of the macro-erosion linear dependence is the same for fixed cooling conditions and a given electrode for all magnetic field values. The results presented in this paper could be taken as a contribution of erosion studies to a better understanding of the mechanisms of spot behavior in gas arcs, as well as to minimizing erosion in electric arc devices.

ACKNOWLEDGMENTS

The authors gratefully acknowledge Professor R. A. Clemente for valuable help in proofreading the manuscript and A. A. B. do Prado for the technical assistance.

The work was supported by CNPq, FAPESP and FINEP of Brazil.

[1] A. Marotta and L. I. Sharakhovsky, J. Phys. D **29**, 2395 (1996).
[2] M. G. Fey and J. McDonald, *Proceedings of the A.I.Ch.E Plasma Chemical Processing Symposium 1976*, edited by D. M. Benenson and E. Pfender (American Institute of Chemical Engineers, New York, 1979) Symp. Ser. 75 (No. 186), pp. 31–37.
[3] V. I. Rakhovsky, IEEE Trans. Plasma Sci. **PS-4**, 81 (1976).
[4] A. E. Guile and B. Jüttner, IEEE Trans. Plasma Sci. **8**, 259 (1980).
[5] A. Marotta and L. I. Sharakhovsky, IEEE Trans. Plasma Sci. **25**, 905 (1997).
[6] A. M. Esipchuk, A. Marotta, and L. I. Sharakhovsky, Inzh.-Fiz. Zh. **73**, 1245 (2000) (in Russian).
[7] A. M. Esipchuk, A. Marotta, and L. I. Sharakhovsky, Inzh.-Fiz. Zh. **74**, 198 (2001) (in Russian).
[8] B. Jüttner, J. Phys. D **34**, R103 (2001).
[9] S. Coloumbe and J-L Meunier, IEEE Trans. Plasma Sci. **47**, 913 (1997).
[10] A. I. Sudarev and A. N. Timoshevski, in *Collection: Thermophysical Investigations*, edited by S. S. Koutateladze, Institute of Thermal Physics of Siberian Department of SU Academy of Siences, 1977, pp. 94–98 (in Russian).
[11] A. S. Anshakov, A. N. Timoshevski, and E. K. Urbakh, Ann. Siberian Department of SU Acad. Sci. Ser. Techn. Sci. **7**, 65 (1988) (in Russian).